A Computational Protocol to Calculate the Phosphorescence Energy of Pt (II) Complexes: Is the lowest triplet excited state always involved in emission? A Comprehensive Benchmark Study

Prashant Kumar[a], *Daniel Escudero* [a]*

[a] Quantum Chemistry and Physical Chemistry Section, Department of Chemistry, KU Leuven, Celestijnenlaan 200F, B-3001 Leuven, Belgium

***Corresponding author**

Email address: daniel.escudero@kuleuven.be – Tel. +32 16 19 33 53

KEYWORDS: DLPNO-CCSD(T), DFT, OLEDs, Phosphors, Pt (II) complexes

ABSTRACT

The reliable calculation of the phosphorescence energies of phosphor materials is at the core of designing efficient phosphorescent organic light-emitting diodes (PhOLEDs). Therefore, it is of paramount importance to have a robust computational protocol to perform those calculations in a black-box manner. In this work, we use Domain Based Local Pair Natural Orbital Coupled Cluster theory with single, double and perturbative triple excitation (DLPNO-CCSD(T)) calculations to attain the phosphorescence energies of a large pool of Pt (II) complexes. Several approaches to incorporate relativistic effects in our calculations were tested. In addition, we have used the DLPNO-CCSD(T) values (i.e., our best theoretical values) to assess the performance of different flavors of density functional theory including pure, hybrid, meta-hybrid, and range-separated functionals. Among the tested functionals, the M06HF functional provides the best values as compared with the DLPNO-CCSD(T) ones, with a mean absolute deviation (MAD) value of 0.14 eV. In its turn, and thanks to the increased accuracy achieved in the calculation of phosphorescence energies, we also demonstrate that not all the investigated complexes emit from their lowest lying triplet-state (T_1). The outlier complexes include different complex photophysical scenarios and both Kasha and anti-Kasha types of complexes. Finally, we provide a general computational protocol to pre-screen whether T_1 is actually the emissive state and to accurately calculate the phosphorescence energies of Pt (II) complexes.

1. INTRODUCTION

Over the past few years phosphorescent organo-transition metal complexes have been used extensively in modern electro-optical technologies such as e.g., organic light-emitting diodes (OLEDs)[1], photocatalysis[2], light-emitting electrochemical cells (LECs)[3], optical sensors[4], dye-sensitized solar cells[5], in-vivo imaging[6] and also in artificial photosynthesis[7]. Especially in the context of OLEDs, organo-transition metal complexes have merged as a popular contender due to their low-cost fabrication and excellent optical, electrical and photophysical properties. The central heavy atom present in these complexes induces large spin-orbit couplings (SOCs) which results in efficient intersystem crossing (ISC) and ultimately leads to an efficient conversion of electrical charges into excitons[8,9].

Quantum chemical modelling of the photophysical properties of phosphors is a fundamental ingredient for the design of tailored phosphors for OLEDs[10–15]. For a long time, canonical coupled-cluster method with singlet, doublet and perturbative triplet excitations, i.e., CCSD(T), has been considered the golden standard in the hierarchy of coupled cluster methods.[16] However, because of its large computational cost, its applicability was limited to small-size molecular systems. The recent developments on low-order scaling approximations to CCSD(T), such as e.g., the Domain Based Local Pair Natural Orbital Coupled Cluster theory with single, double and perturbative triple excitations, i.e., DLPNO-CCSD(T)[17–20], have enabled the treatment of medium-size molecular systems amounting up to a few hundreds of atoms. All in all, in view of their near-linear scaling features, efficiency and accuracy, the DLPNO-CCSD(T)[19] method has become the state-of-the-art golden standard method to calculate in an accurate and reliable manner, the molecular electronic energies and properties for medium-size molecular systems. These methods were recently expanded to be able to treat open-shell systems[21] and thus opening the door to the calculation of

phosphorescence energies for molecular systems. Here, the performance of the DLPNO-CCSD(T)[20] method to calculate phosphorescence energies in phosphors is assessed for the first time.[22–25]

The calculation of accurate phosphorescence energies has been proven difficult for Pt (II) complexes.[26,27] Many pseudo-square planar Pt (II) complexes displaying various cyclometalating and ancillary ligands have been synthesized and characterized in the literature. Their photophysical properties have been the scope of multiple investigations.[28–31] Square-planar Pt(II) complexes often possess very complex and rich photochemical properties,[32,33] such as anti-kasha emission but also dual photoluminescence.[34–37] These complex photochemical scenarios make difficult the development of computational protocols enabling the calculation of the phosphorescence energy of a given arbitrary Pt(II) complex without prior information on its measured photophysical properties. Thus, in this contribution, we firstly aim at benchmarking state-of-the-art methods for the phosphorescence energies of Pt(II) complexes and secondly to devise strategies to systematically assess whether the lowest triplet excited state minimum is involved in the emission processes or not. The pool of complexes studied here include i) complexes which emit from their lowest lying triplet-state, that are kasha-like complexes (Case I complexes in Figure 1); ii) complexes emitting from higher lying triplet excited states, that are anti-kasha complexes (Case II complexes) and iii) complexes characterized by close-lying triplet states (Case III complexes).

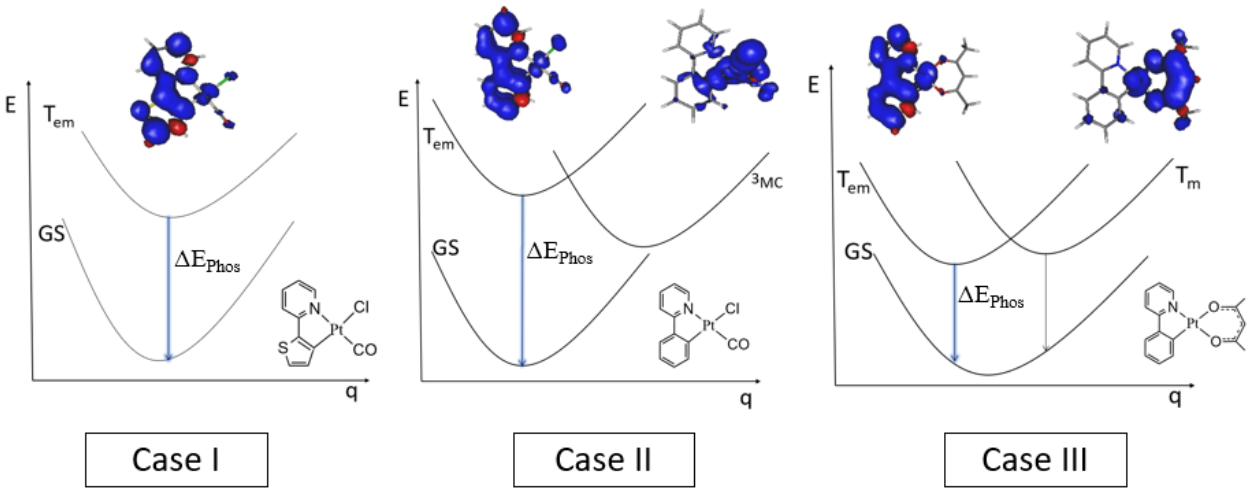

Figure 1. Simplified Jablonski energy diagram depicting the ground state (GS) and the triplet emissive excited states involved in the photophysics of these complexes; including e.g., the excited state involved in emission, T_{em}; the metal-centered triplet excited state, ^3MC; and a higher-lying triplet excited state, T_m.

2. COMPUTATIONAL DETAILS

All the ground state geometries of the Pt (II) complexes shown in Figure 2 were optimized with density functional theory (DFT)[38–40] using the B3LYP functional[41–43] in combination with the 6-31G* basis set for all atoms and the MWB60[44] pseudopotential for the platinum atom. In addition, optimizations of both the first and higher-lying triplet states were performed with time-dependent DFT (TD-DFT)[45–48] using the same functional and basis sets as in the DFT calculations. In a systematic way, the geometries of the first three lowest triplet excited states (T_1-T_3) were optimized with TD-DFT for all the complexes. In the case of the T_1 states, UB3LYP geometry optimizations using the same functional and basis sets as in the DFT calculations were also performed. The Gaussian16[49] program package was used for the optimizations.

For the phosphorescence energies both ΔSCF and linear-response TD-DFT calculations were tested. The vertical phosphorescence energies correspond to the TD-DFT emission energies calculated at their optimized triplet excited state minima (T_1-T_3). Conversely, the ΔSCF values correspond to the difference between the triplet and singlet single point energy calculations at these optimized triplet minima. The DLPNO-CCSD(T) phosphorescence energies are thus based on the ΔSCF approach. For the latter calculations, both def2-nZVP and correlation-consistent cc-PVnZ type basis sets for light atoms were tested. In these calculation the def2-ECP pseudopotential for Pt was used. For the the DLPNO-CCSD(T) calculations, tight Pair Natural Orbital (PNO) settings (TCutPairs = 10^{-5}, TCutPNO = 1×10^{-7}, TCutMKN = 10^{-3}) and very tight SCF (energy change 1×10^{-9} au) settings were used to reach negligible numerical noise in the calculations. To account for relativistic effects we assessed different approaches. Specifically; and besides the pseudopotential approach as described above, DLPNO-CCSD(T) calculations were also performed in combination with two-component Hamiltonians, such as the Douglas-Kroll-Hess (DKH)[50] and Zero-Order-Relativistic-Approximation (ZORA)[51,52] Hamiltonians. The latter calculations were performed in combination with relativistic-contracted basis sets, i.e., def2-nZVP-DK and cc-PVnZ-DK. The DLPNO-CCSD(T) calculations were performed with the ORCA 4.1[53] program package.

In addition, vertical TD-DFT and ΔSC-DFT calculations were performed to assess the performance of DFT-based methods for the phosphorescence energies of Pt(II) complexes. These calculations were performed at the optimized triplet excited state minima (T_1-T_3). Additionally, TD-DFT calculations were also performed with and without Tamm-Dancoff approximation (TDA)[54] which is known to remarkably improve the problematic triplet instability in TD-DFT.[55–57] Different xc functionals including pure functionals (BP86[58,59], B97D[60]), range-separated hybrid

functionals (CAM-B3LYP[61], LC-wPBE[62]), hybrid functionals (B3LYP[41,42], PBE0[63]), meta-hybrid functionals (M06L[64], M062X[65], M06[65], M06HF[66,67], MN15[68]) and double-hybrid functionals (B2PLYP[69], PW6B95[70]) were tested. All the vertical TD-DFT and ΔSCF-DFT calculations were performed in combination with the 6-311G* basis set along with the MWB60 pseudopotential for Pt using Gaussian16. [49] Both gas-phase and solvent corrected values were computed. The latter calculations made use of the solvation model based on density (SMD).[71] The solvent corrections were extrapolated from the ΔSCF-DFT values to the DLPNO-CCSD(T) ones (see the discussion in the SI and Table S3).

Finally, to assess the performance of the different methods we have used three statistical error descriptors, i.e., i) Mean-absolute deviations (MAD), ii) Mean-signed Deviations (MSD) and iii) Root-mean square deviations (RMSD). Further details can be found in the SI.

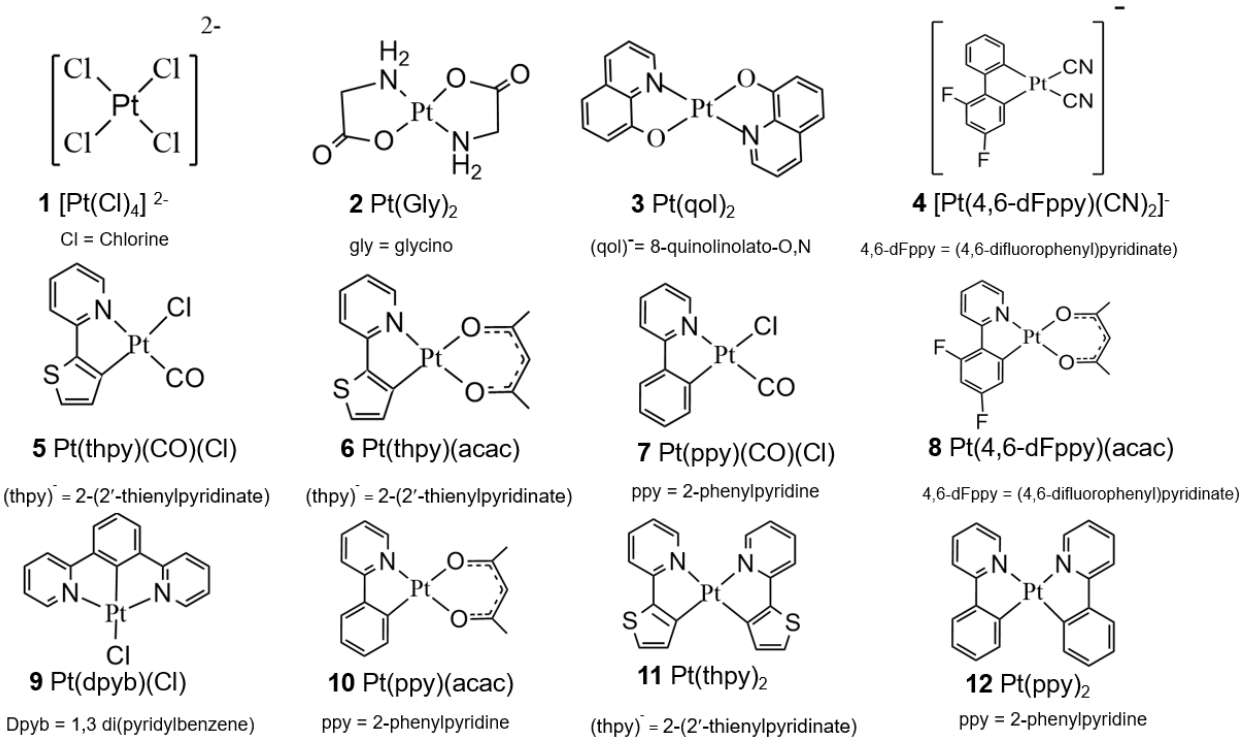

Figure 2. Pseudo square planar Pt (II) complexes under this study

3. RESULTS & DISCUSSIONS

We have studied twelve Pt (II) complexes (see Figure 2), which have been the object of many photophysical investigations, and for which extensive experimental data is available. The small complex **1** was solely chosen to assess the performance of different coupled-cluster approaches and the different ways to introduce relativistic effects in the calculations. The photophysical properties of the rest of the complexes have been systematically and exhaustively investigated by Yersin and coworkers at different temperature regimes and environments.[28] First, we discuss the performance of canonical CCSD(T) versus DLPNO-CCSD(T) for the smallest complex in our benchmarking set, i.e., **1**. Then we proceed to discuss the performance of the DLPNO-CCSD(T) method for complexes **2**-**12**. Finally, various DFT-based approaches to calculate the phosphorescence energy were assessed. A discussion of the overall performance of the latter approaches follows, with general recommendations for end users.

3.1. Canonical CCSD(T) versus DLPNO-CCSD(T). The small complex **1**[72] was selected to test several coupled-cluster approaches, namely canonical CCSD(T) *versus* DLPNO-CCSD(T), for the calculation of its phosphorescence energy. Table 1 collects these results. The experimental emission maximum measured in the single-crystal amounts up to 1.59 eV, and this value is also included in Table 1.[72] Our best theoretical estimators for the phosphorescence energy of **1**, i.e., the CCSD(T) values with both cc-pVQZ and def2-QZVP basis sets render gas-phase values of 1.44, 1.45 and 1.56 eV when combined with pseudopotentials, DKH and ZORA Hamiltonians; respectively. Overall, there is a good agreement between the experimental and the theoretical results regardless of the approach used to account for the scalar relativistic effects, with errors of ca. 0.10 eV with respect to the experiment. Note that the experimental value is measured in the single crystal as the maximum of the emission band which results from vibronic couplings. Given

that the computed value is obtained in the gas phase and that vibronic couplings are not included in the calculations, we therefore cannot conclude which relativistic approach is best for these types of complexes. The results shown in Table 1 also highlight that using TZ-quality basis sets render very similar values with those obtained with QZ-quality basis sets (within 0.04 eV), and therefore because of computational ease the former basis set was systematically used for complexes **2**-**12**.

Next, we tested the performance of DLPNO-CCSD(T) against canonical CCSD(T). The DLPNO-CCSD(T) calculations made use of different settings. Specifically, the TightPNO and NormalPNO settings were tested. Both TightPNO and NormalPNO were used in combination with pseudopotentials while only TightPNO was used in combination with DKH and ZORA Hamiltonians. Comparing TightPNO versus NormalPNO, the former clearly outperforms the latter. Specifically, the NormalPNO values are underestimated by ca. 0.05-0.1 eV with respect to the TightPNO ones (see Table 1); so that the latter approach is chosen as the default setting to study complexes **2**-**12**. We note that, regardless of the basis set used, the combination of DLPNO-CCSD(T) with ECPs leads to very similar values with respect to the combination of CCSD(T) with ECPs (e.g., compare 1.46 eV vS 1.44 eV for a QZ-basis set in Table 1); and thus, giving validity to the computed DLPNO-CCSD(T) values. Conversely, the comparisons of the values obtained with DLPNO-CCSD(T) with DKH/ZORA vS CCSD(T) with DKH/ZORA reveals that the former approaches tend to overestimate the computed values by 0.1 eV. Among the different relativistic approaches, the DKH value perfectly matches the experimental one while the pseudopotential (ZORA) approach one tends to underestimate (overestimate) the experimental one (see Table 1).

Table 1. Calculated CCSD(T) and DLPNO-CCSD(T) values (in eV) for the phosphorescence energy of complex **1**.

Basis Sets	**CCSD(T) with ECP**	**CCSD(T) with DKH**	**CCSD(T) with ZORA**	**DLPNO-CCSD(T) with ECP**		**DLPNO-CCSD(T) with DKH**	**DLPNO-CCSD(T) with ZORA**	**Exp.**
				Normal PNO	Tight PNO	Tight PNO	Tight PNO	
Def2-SVP	1.53	1.55	1.67	1.53	1.58	1.66	1.77	1.59
Def2-TZVP	1.45	1.48	1.59	1.45	1.50	1.59	1.70	
Def2-QZVP	1.44	1.45	1.56	1.44	1.46	1.57	1.68	
cc-pVDZ	1.50	1.52	1.63	1.50	1.55	1.63	1.73	
cc-pVTZ	1.45	1.48	1.58	1.44	1.50	1.58	1.69	
cc-pVQZ	1.44	1.45	1.56	1.39	1.46	1.56	1.67	

[a] Experimental value in eV from Ref. 72

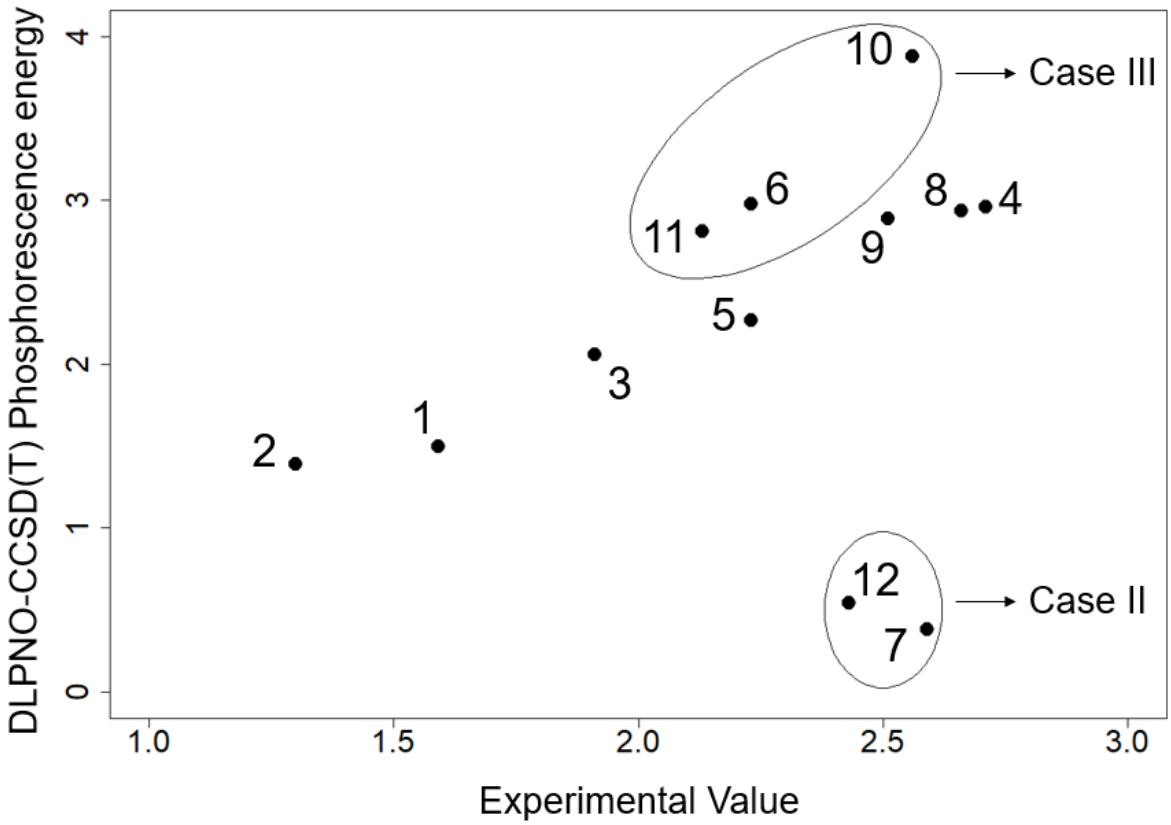

Figure 3: Comparison of DLPNO-CCSD(T) phosphorescence energies (in eV) calculated at the lowest triplet state geometry (UB3LYP-T_1) vs the experimental ones (in eV).[28,72,73]

3.2 Phosphorescent energy calculations in complexes 1-12: In the previous section we benchmarked several CC approaches for complex **1**. The above investigations enable us to choose an optimal computational protocol in terms of still being affordable for medium-size molecular systems, such as complexes **2-12**, but that still guarantees accurate phosphorescence energy calculations. Specifically, we verified that for the DLPNO-CCSD(T) calculations a TZ-quality basis sets guarantees enough accuracy and that TightPNO should preferentially be used instead of NormalPNO settings criteria. Thus, in complexes **2**-**12**, TightPNO was used for the DLPNO-CCSD(T) calculations in combination with def2-TZVP and correlation consistent cc-PVTZ basis sets. As no conclusive results were obtained for **1** in terms of the preferred approach to account for

relativistic effects, we herein tested all possibilities for **2**-**12**. Note also, that for the calculation of the phosphorescence energies, the common approach in the community consists of obtaining the optimal geometry of the lowest triplet excited state (T_1), with UDFT or TD-DFT, followed by ΔSCF calculations (with e.g., the DLPNO-CCSD(T) method) or a vertical TD-DFT calculation at this geometry. Thus, in a first step, we optimized the geometries of T_1 with UB3LYP for complexes **2-12** and we next calculated the DLPNO-CCSD(T) phosphorescent energies (TightPNO, def2-TZVP basis sets in combination with the def2-ECP pseudopotential for Pt) at these geometries. In Figure 3 is shown a comparison of the DLPNO-CCSD(T) phosphorescence energies for **2-12** versus the experimental values. Clearly, the DLPNO-CCSD(T) values match the experimental ones for the majority of compounds, see e.g., complexes 1[72], 2[73], 3[74], 4[75], 5[76], 8[77] and 9[78] in Figure 3. These complexes which are; in view of these evidences, emitting from their lowest triplet excited state (T_1 and thus show Kasha-like emission), are classified here as Case I complexes. A quick inspection of Figure 3 also reveals that there are complexes that behave as outliers. For some of the outliers, the DLPNO-CCSD(T) phosphorescent energies are underestimated by 2 eV with respect to the experimental values (see complexes 7 and 12; which are classified here as Case II complexes) while for some other complexes their computed values are overestimated by up to 1.5 eV (see 11, 6, and 10; Case III complexes). Given the expected accuracy of DLPNO-CCSD(T) for the phosphorescence energies of these complexes, these results highlight that Case II and Case III complexes likely possess complex photochemical scenarios; where T_1 is likely not the emissive state and/or the optimal T_1 local minimum structure obtained with UB3LYP is not the geometry involved in the emission of these complexes. In Figure 4 are shown the optimized S_0 and T_1 geometries for selected complexes, namely two Case I complexes (1 and 5); one Case II complex (7) and one Case III complex (10). In addition, the optimized geometry of the actual emissive state

(T_{em}) for the Case II-III complexes is also shown in Figure 4 for completeness. The spin density distributions of the T_1 and T_{em} states are also plotted in Figure 4. In the SI, are found the optimized geometries and spin density distribution plots for the rest of complexes. Let us first discuss Case I complexes. For the latter complexes, their S_0 and T_1 optimized geometries are rather similar; being the main geometrical rearrangements when moving from S_0 to T_1 the change in some of the Pt-ligand bond distances (see Figure 4). The spin density plot of their T_1 states highlights the predominant metal-to-ligand charge transfer (^{3}MLCT) character for the complexes (e.g., 5) with the exception of that of complex 1, which can be better described as a mixed ^{3}MC/^{3}MLCT/^{3}LC state. For Case II complexes a UB3LYP optimization of the lowest triplet excited state leads to a metal-centered state (i.e., ^{3}MC), as clearly highlighted by inspecting their spin density distribution plot (see e.g., for complex 7 in Figure 4). Conversely to Case I complexes, the optimized S_0 and T_1 geometries for Case II complexes are rather different, being the main difference the transition from the typical square-planar coordination at S_0 to a tetrahedral-like coordination at T_1 (see e.g., a change from 180° to 111° in the dihedral angle between the ligand planes). As one of us has previously described for similar square-planar Pt(II) complexes, ^{3}MC complexes[79] are not involved in emission but rather in nonradiative deactivation channels. More in details, in the vicinity of the ^{3}MC well there is a minimum energy crossing point between the S_0 and the ^{3}MC potential energy surfaces that facilitates the nonradiative decay and the recovery of the S_0 geometry without the emission of a photon. The fact that ^{3}MC is not involved in emission[79] is also reflected in the large disagreement between the experimental and DLPNO-CCSD(T) values from T_1 (see e.g., in Figure 3 that the computed values are underestimated by ca. 2 eV). Accordingly, the measured photoluminescence quantum yields for Case II complexes are rather low (e.g., <0.01 for **12**)[80]. It seems thus, that higher-lying excited states (i.e., T_m where m>1) are responsible for the

experimentally measured phosphorescence in these complexes. Therefore, we explored the potential energy surfaces of higher-lying excited states of Case II complexes with TD-DFT calculations. For instance, the optimized geometry of the triplet excited state which is likely involved in emission for complex 7 corresponds to T_2 (see T_{em} in Figure 4). The optimal geometry of T_{em} is very similar as the one of S_0 and its spin density distribution plot reveals a predominant ^{3}MLCT character. In addition, the computed DLPNO-CCSD(T) phosphorescence energy at T_{em} (2.80 eV) is in a much better agreement with the experimental one (2.59 eV). Under all these circumstances we are quite confident that this higher-lying excited state is the state involved in emission for 7. Same conclusions are obtained for complex 12 (see in Table S2 the computed values). Note that the anomalous emission in Case II complexes, although here classified as anti-Kasha emission, cannot be strictly categorized as a truly anti-Kasha emission because for instance for 7, the T_2 state, at its optimized geometry, is the lowest triplet excited state.

We now turn the discussion to Case III complexes. A simple exploration of their T_1 geometries, and spin density distribution plots (see e.g., for complex 10 in Figure 4) may in principle not raise any suspicion that these states are not responsible for the experimentally observed emission for these complexes. However, the computed DLPNO-CCSD(T) phosphorescence energies at their optimized T_1 geometries reveal strong disagreements with their experimental counterparts (i.e., the computed values are generally overestimated for Case III complexes, e.g., by up to ca. 1.3 eV in the case of complex 10 where the phosphorescence energy computed at T_1 is 3.88 eV and the experimental one is 2.56 eV). Given the expected accuracy of DLPNO-CCSD(T), this likely means that the optimal T_1 local minimum structure obtained with UB3LYP is likely not the geometry involved in the emission of these complexes. The excited state potential energy surfaces of Pt(II) complexes are rather complicated, leading in some cases to unusual photophysics, as dual or

multiple emissive scenarios and/or temperature or excitation wavelength-dependent emission switch[10,37]. Therefore, we also explored the higher-lying triplet excited state potential energy surfaces of case III complexes with TD-DFT calculations. For instance, in the case of complex 10, while the computed phosphorescence energy at the T_1 geometry is 3.88 eV the one computed at the T_2 geometry is 2.81 eV. An inspection of the spin density distribution plots reveals that T_1 and T_2 are both of predominant ^{3}MLCT character, but interestingly they involve different ligand-based orbitals (see Figure 4). Specifically, T_1 involves the *acac* ligand while T_2 involves the *ppy* ligand. Additionally, the geometrical parameters of the T_2 minimum, such as e.g., platinum-ligand bond distances and planarity, resemble more those of the S_0 minimum than in the case of T_1. Furthermore, adiabatically T_2 is lower in energy than T_1 (see the relative adiabatic energy differences in Table S2). Under all these circumstances we are quite confident that T_2 is the state involved in emission for **10**. Same conclusions are obtained for complexes 11 and 6; for which the close-lying TDDFT-T_1 minima, but not the UB3LYP-T_1 optimized minima, are likely responsible for their emissive features (see their computed phosphorescence energies and relative adiabatic energetic differences in Table S2). Dual photoluminescence is not uncommon for these complexes; likely arising from a thermal equilibrium between triplet excited states. For instance, related complexes of the parent complex 10, have been reported to exhibit chameleonic emissive properties, which are finely tuned by external stimuli such as solvent and temperature.[37] All in all, the prediction of the phosphorescence properties for Case III complexes is challenging. The results for complexes 6, 10, 11 highlight that the lowest adiabatic triplet state is likely the one involved in the emission processes (see their relative adiabatic energy differences in Table S2). However, one cannot disregard that this is always the case for any given complex; as e.g., a significant activation barrier between different triplet excited states might prevent the population of the lowest adiabatic

triplet state at a given temperature. This situation has been described on related platinum-butterfly complexes.[81]

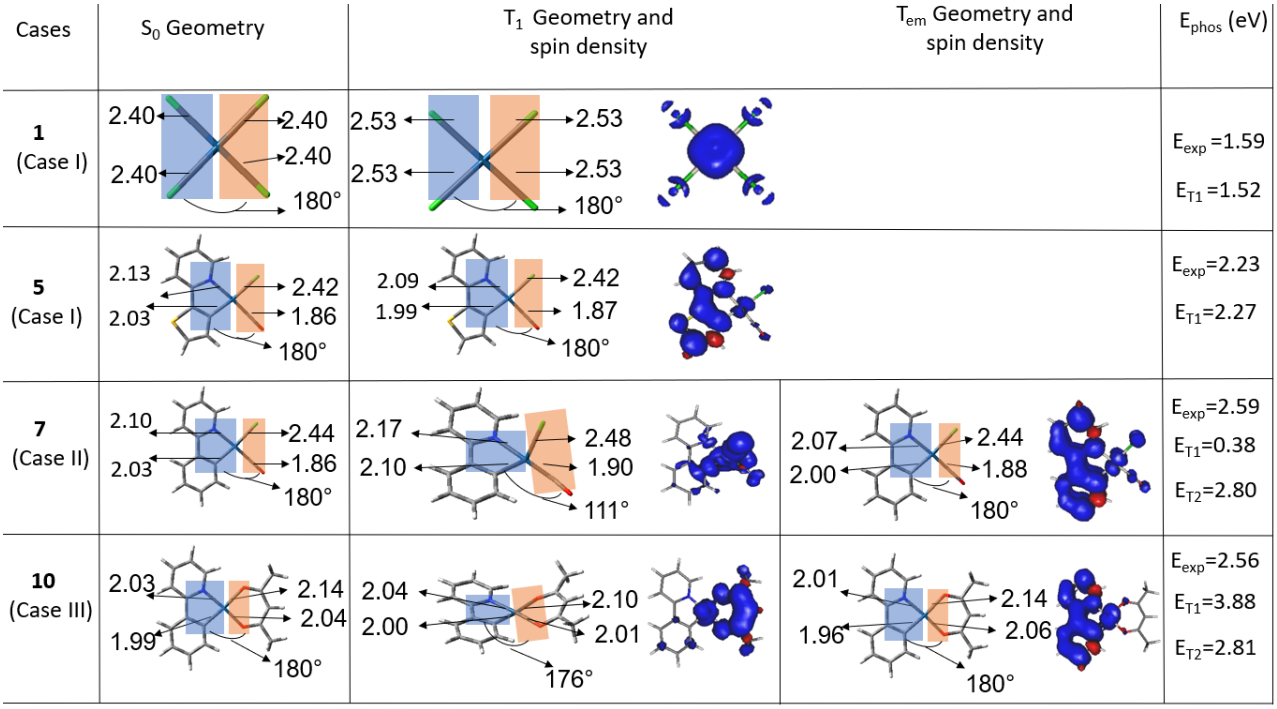

Figure 4: Comparison of geometrical parameters of the optimized geometries of S_0, T_1 and T_{em} along with spin density plots for the T_1 and T_{em} states of complexes 1, 5, 7 and 10 along with the computed and experimental phosphorescence energies. Bond distances are given in Å.

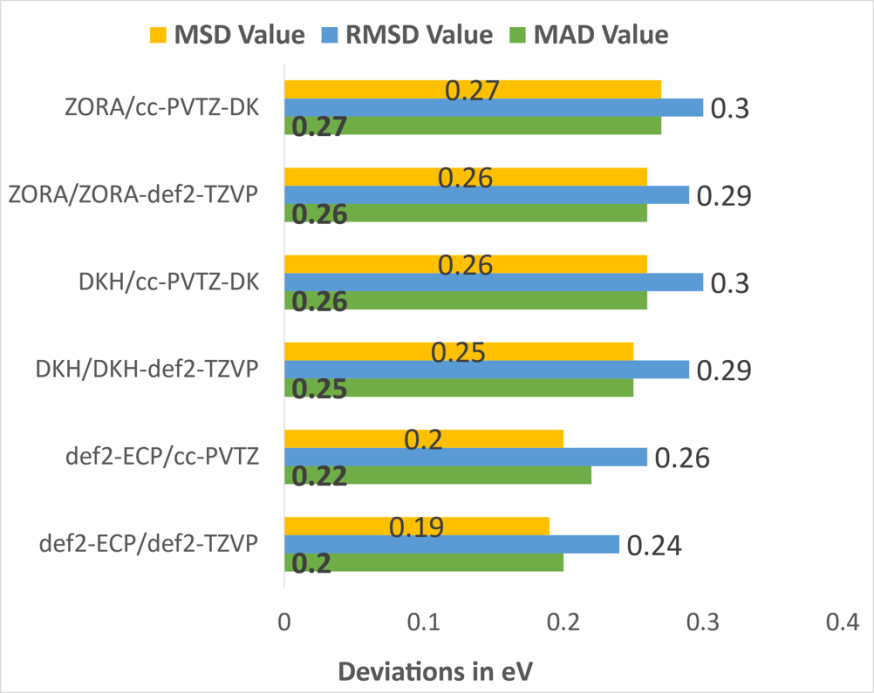

Figure 5. Deviations of different DLPNO-CCSD(T) approaches (gas phase) for the phosphorescence energies of complexes 1-12 with respect to the experimental values (in eV).[28,72,73]

After reassigning the actual triplet excited state involved in the emission for complexes 6, 7, 10, 11 and 12; i.e., the T_{em} state, we are now ready to discuss the statistical errors (i.e., mean absolute deviation (MAD), the mean signed deviation (MSD) and the root-mean-square deviation (RMSD) values) of the different DLPNO-CCSD(T) approaches for the phosphorescence energies of complexes **1**-**12**. The statistical errors are shown in Figure 5. The experimental value was used as reference. Note that the experimental values are obtained as the maximum of the emission band and in the presence of solvent. In this regard, implicit solvation models in combination with DLPNO-CCSD(T) have not been implemented yet. Thus, in order to assess the effect of solvation on the computed phosphorescence energies we extrapolated the solvent corrections from the SMD-ΔSCF calculations. As seen in Table S3 the solvent corrections are well below 0.06 eV for all the

complexes, and thus they are neglected here in the calculation of the statistical errors. Among the tested DLPNO-CCSD(T) schemes, the pseudopotential approach combined with the def2-TZVP basis set provides the best statistical errors (MAD = 0.20; RMSD = 0.24 and MSD = +0.19). Note that regardless of the used computational protocol, the DLPNO-CCSD(T) results are systematically overestimated with respect to the experimental values (see positive MSD values in Figure 5). The combination of two-component Hamiltonians with DKH-def2-TZVP and cc-PVTZ-DK basis sets leads to slightly larger divergences with respect to the experimental values. We recall that similar trends were observed for **1**. All in all, regardless of the protocol used, these errors are within the expected range of accuracy of the DLPNO-CCSD(T) method.[21] The DLPNO-CSSD(T) values will serve us in the next section as best theoretical estimators to benchmark several DFT-based approaches.

To finish the discussion, we propose in the following a computational protocol to assess whether the lowest triplet excited state (T_1) is involved in the emission of these type of complexes. Such a protocol might help to computationally pre-screen the actual emitting state of an arbitrary Pt(II) complex. TD-DFT optimizations of the three lowest triplet excited states should systematically be performed followed by the calculation of the DLPNO-CCSD(T) phosphorescent energies at these geometries. If T_1 remains the lowest excited state after relaxation and the T_m states are adiabatically located significantly higher in energy (>0.1 eV) one can safely conclude that the complex will likely emit from T_1 (Case I complexes). Case II complexes are easily recognizable, as the computed DLPNO-CCSD(T) phosphorescent energies are typically very small (well below 1 eV), their optimal geometries are fully distorted and a simple plot of the spin-density distribution unambiguously displays ^{3}MC character, such as e.g., in complexes 7[82] and 12[80]. For Case II complexes, the triplet state which is adiabatically the lowest excited state (excluding the ^{3}MC state)

is likely the state involved in emission. Finally, for Case III complexes the assignment of the emissive state is more cumbersome because they likely possess similar phosphorescence energies from several triplet states and possibly small adiabatic energetic differences between these states. For these complexes, as observed here for complexes 6[83], 10[84] and 11[85], the triplet state which is adiabatically the lowest triplet excited state is likely the one involved in emission. As mentioned above, the phosphorescence properties of Case III complexes are prone to be subtly modulated by external stimuli. This is specially true in the case that the relative adiabatic energy difference is small enough (<0.1 eV), so that thermal equilibrium between the triplet excited states is possible. For complexes 6, 10 and 11; and in view of the computed relative adiabatic energy differences between triplet states (see Table S2); these complexes are unlikely to possess chameleonic emissive properties.

3.3 Performance of DFT-based approaches for the phosphorescent energies. Next, we assess the performance of DFT-based approaches to calculate the phosphorescent energies. We have used three different approaches: i) T_{em} (using ΔSCF-DFT): corresponding to the energy difference between the singlet state and the lowest triplet state at the T_{em} optimized geometry; ii) T_{em} (using TD-DFT): This is the vertical emission energy from the emissive triplet state of interest at its optimized geometry to the ground state calculated using TD-DFT; and iii) T_{em} (using TDA-TDDFT): This is the vertical emission energy from the emissive triplet state of interest at its optimized geometry to the ground state calculated using TDDFT with Tamm-Dancoff approximation (TDA). In addition, the performance of different flavors of DFT, i.e., from pure, hybrid, meta-hybrid to range-separated functionals, for the phosphorescence energies of **1**-**12** have been assessed within the three different approaches.

As mentioned above, the DLPNO-CCSD(T)/def2-TZVP values are our best theoretical estimators and are used herein as reference. The results for the different xc functionals are presented in Figure 6 and in Tables S5-S6. Overall, and regardless the chosen xc functional, the ΔSCF-DFT values (black dots in Figure 6) are closer to the reference DLPNO-CCSD(T) values. TDA-TDDFT (red dots) and TD-DFT (green dots) are generally less accurate than ΔSCF-DFT for the phosphorescence energies of the studied Pt (II) complexes. Specially, in the case of range-separated functionals (see e.g., CAM-B3LYP and LC-WPBE in Figure 6) the TD-DFT values are significantly underestimated (by more than 1 eV in the most extreme cases). In the latter cases, the use of TDA with TDDFT has a significant impact on the results. Specifically, by neglecting all the deexcitation processes within the TDA formalism it corrects for the unphysicalities observed with TDDFT. This trend has been previously described for the triplet excited states of organic molecules.[56] Conversely, in the case of pure functionals (see e.g., BP86 in Figure 6), the impact of the used DFT-based approach on the results is negligible. Finally, in case of hybrid functionals (e.g., B3LYP and PBE0 in Figure 6), and meta-hybrid functionals it is less evident to extract general conclusions about the performance of the different DFT-based approaches. For instance, in the case of hybrid functionals, while the TDA-TDDFT approach outperforms the other two approaches for **5**, **6** and **11**, ΔSCF-DFT appears superior for the rest of compounds. Different functionals and approaches perform better in some specific situations and for some types of excited states. For instance, for compounds emitting from a triplet excited state with predominant ^{3}MC character (such as e.g., **1** and **2**), the ΔSCF-DFT approach is always performing significantly better than the other two approaches and the use of TDA within TD-DFT does not lead to a significant improvement of the results as compared to the standard TDDFT approach.

Overall, all the tested DFT-based approaches (with the caveat of the M06HF functional) underestimate the phosphorescent energies as compared with the reference DLPNO-CCSD(T) values. Among the different DFT-based approaches, our results highlight that the ΔSCF-DFT approach is suited to calculate the phosphorescent energies of Pt(II) complexes, and it is thus recommended here. Among the different TDDFT approaches, TDA-TDDFT outperforms TDDFT. The latter results are aligned with previous investigations.[55–57]

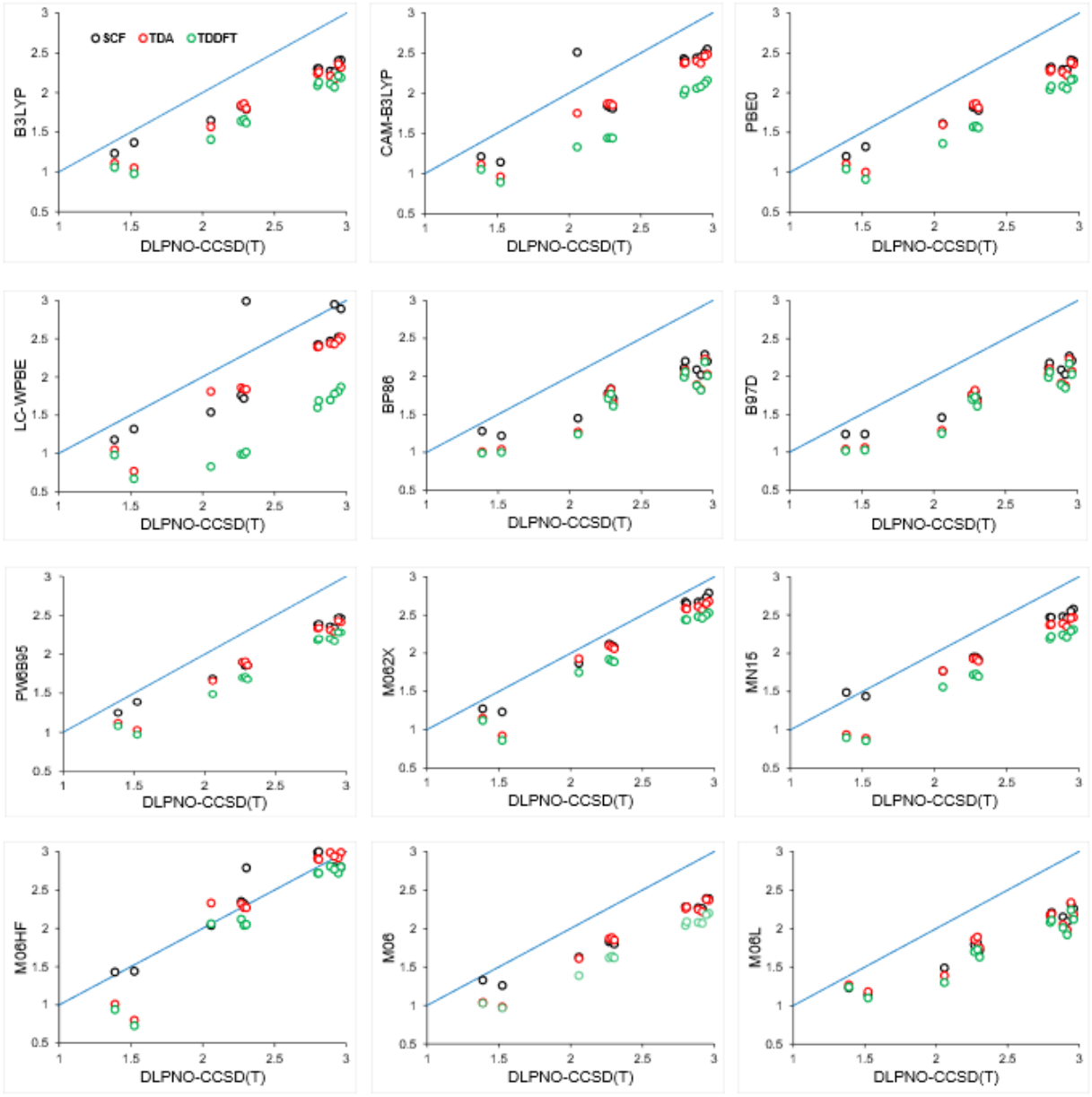

Figure 6. Comparison of the phosphorescence energies values (in eV) calculated with various DFT-based approaches i.e. ΔSCF-DFT (black dot), TDDFT (green dot) and TDA-TDDFT (red dot) with respect to the reference DLPNO-CCSD(T) values.

As mentioned above, the ΔSCF-DFT approach is best suited for calculating the phosphorescence energies of Pt(II) complexes. Now we test the performance of the various xc functionals in combination with the ΔSCF-DFT approach. The statistical errors are presented in Figure 7. The M06HF functional, a meta GGA-hybrid functional is performing best, with a MAD value of 0.14 eV (reference values are the DLPNO-CCSD(T) ones) and a MSD value of +0.08 eV. Notably, this is the only functional that slightly overestimates the phosphorescence energies; while the rest of tested xc functionals tend to underestimate the phosphorescence energies (see negative MSD values in Figure 7). In terms of performance, other Minnesota functionals, such as e.g., M062X and MN15 with MAD value of 0.19 and 0.32 eV, respectively; come after M06HF. The above meta-hybrid functionals possess different amounts of HF exchange. Specifically, M06HF, M062X and MN15 possess 100%, 54% and 44% of HF exchange; respectively. The results highlight that amount of %HF exchange has a great impact on the quality of the ΔSCF-DFT results for the phosphorescent energies. Specifically, those functionals bearing a larger amount of %HF exchange perform best, such as e.g., M06HF (for a comparison of all Minnesota functionals see Figures S4-S6). The statistical errors for the rest of functionals are also presented in Figure 7. The range-separated functional LC-wPBE, with a MAD value of 0.37 eV, comes next in terms of performance. Then, the double hybrid PW6B95 functional, with a MAD value of 0.40 eV, follows. Similar performances are obtained with global hybrid functional, such as e.g., B3LYP (MAD = 0.46 eV) and other range-separated functionals, such as e.g., CAM-B3LYP (MAD = 0.44 eV). Pure functionals, such as e.g., BP86 (MAD = 0.58 eV) and B97 (MAD = 0.59 eV) perform overall

worst for the calculations of the phosphorescence energy of these Pt(II) complexes. Therefore, pure functionals are generally not recommended here.

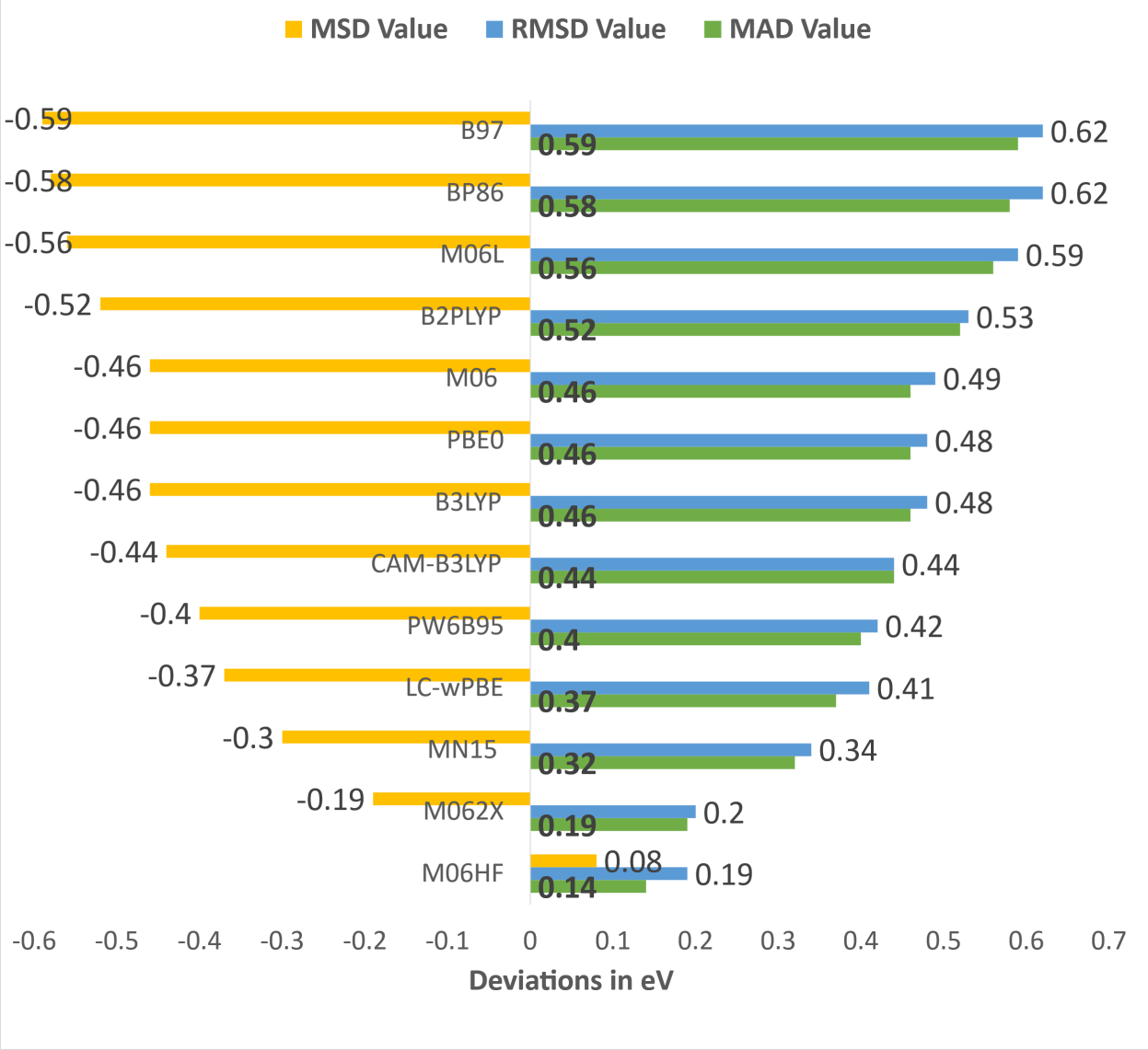

Figure 7. Statistical errors for the phosphorescence energies values (in eV) calculated with various xc functionals in combination with the ΔSCF-DFT approach.

Conclusion

We have presented a comprehensive benchmark study on the calculation of the phosphorescence energies of square-planar Pt (II) complexes. First, we have assessed the performance of the golden-standard DLPNO-CCSD(T) method to compute the phosphorescence energies using different approaches to account for relativistic effects but also using different basis sets and settings within the calculations. To calculate phosphorescence energies the common approach in the community consists of obtaining the optimal geometry of the lowest triplet excited state (T_1) and at this geometry calculate the emission energy with ΔSCF and/or TD-DFT approaches. Here, with the help of the accurate DLPNO-CCSD(T) calculations, we demonstrate that this approach does not always remain valid for all the investigated complexes. For the outlier compounds it is necessary to perform geometry optimizations of higher-lying triplet excited states (i.e., T_1-T_3) to obtain the actual species involved in the emission. These investigations have helped us to classify the Pt(II) complexes in three different classes of complexes, according to their complex photochemical scenario at play. In addition, we provide a computational protocol to assess which is the triplet excited state involved in the emission of any arbitrary Pt(II) complex, and importantly without a prior knowledge of its emission properties. Our study contributes to understand the chameleonic emissive properties often reported in the literature for these type of complexes including multiple emissive scenarios and/or temperature and/or excitation wavelength-dependent emission switch.

Besides, we have also explored different DFT-based approaches to calculate the phosphorescence energies. The ΔSCF-DFT approach is found superior to the TDA-TDDFT and TD-DFT approaches. We have also assessed the performance of different flavors of DFT. Among the various xc functionals tested, meta-hybrid functionals outperform the rest of functionals. The

amount of %HF exchange within the xc functionals strongly impacts the results, being M06HF the best performing functional for the phosphorescence energies of these complexes.

Supporting Information.

The supporting information contains the following data: computed data and statistical error analysis of the data, spin density plots, and xyz-coordinates of the optimized geometries.

ACKNOWLEDGMENT

We acknowledge Daniel Vidal for the preliminary investigations of the complexes. D. E. acknowledges KU Leuven internal funds and FWO.

REFERENCES

(1) Yersin, H. *Highly Efficient OLEDs with Phosphorescent Materials*; John Wiley & Sons, 2008.

(2) Hoffmann, N. Photochemical Reactions as Key Steps in Organic Synthesis. *Chem. Rev.* **2008**, *108* (3), 1052–1103.

(3) Kapturkiewicz, A. Electrochemiluminescent Systems as Devices and Sensors. *Electrochem. Funct. Supramol. Syst.* **2010**, 477–522.

(4) Wang, X.; Wolfbeis, O. S. Optical Methods for Sensing and Imaging Oxygen: Materials, Spectroscopies and Applications. *Chem. Soc. Rev.* **2014**, *43* (10), 3666–3761.

(5) O'regan, B.; Grätzel, M. A Low-Cost, High-Efficiency Solar Cell Based on Dye-Sensitized Colloidal TiO 2 Films. *Nature* **1991**, *353* (6346), 737–740.

(6) Boverman, G.; Shi, X.; Cotero, V. E.; Filkins, R. J.; Srivastava, A. M.; Lorraine, P. W.; Neculaes, V. B.; Ishaque, A. N. Applications of Phosphorescent Materials for In-Vivo Imaging of Brain Structure and Function. In *Clinical and Translational Neurophotonics; Neural Imaging and Sensing; and Optogenetics and Optical Manipulation*; International Society for Optics and Photonics, 2016; Vol. 9690, p 969018.

(7) Zhang, B.; Sun, L. Artificial Photosynthesis: Opportunities and Challenges of Molecular Catalysts. *Chem. Soc. Rev.* **2019**, *48* (7), 2216–2264.

(8) Penfold, T. J.; Gindensperger, E.; Daniel, C.; Marian, C. M. Spin-Vibronic Mechanism for Intersystem Crossing. *Chem. Rev.* **2018**, *118* (15), 6975–7025.

(9) Fleetham, T.; Li, G.; Li, J. Phosphorescent Pt (II) and Pd (II) Complexes for Efficient, High- color- quality, and Stable OLEDs. *Adv. Mater.* **2017**, *29* (5), 1601861.

(10) Escudero, D.; Jacquemin, D. Computational Insights into the Photodeactivation Dynamics of Phosphors for OLEDs: A Perspective. *Dalt. Trans.* **2015**, *44* (18), 8346–8355.

(11) Escudero, D. Quantitative Prediction of Photoluminescence Quantum Yields of Phosphors from First Principles. *Chem. Sci.* **2016**, *7* (2), 1262–1267.

(12) Jacquemin, D.; Escudero, D. The Short Device Lifetimes of Blue PhOLEDs: Insights into the Photostability of Blue Ir (III) Complexes. *Chem. Sci.* **2017**, *8* (11), 7844–7850.

(13) Zhang, X.; Jacquemin, D.; Peng, Q.; Shuai, Z.; Escudero, D. General Approach to Compute Phosphorescent OLED Efficiency. *J. Phys. Chem. C* **2018**, *122* (11), 6340–6347.

(14) Escudero, D. Photodeactivation Channels of Transition Metal Complexes: A Computational

Chemistry Perspective. In *Transition Metals in Coordination Environments*; Springer, 2019; pp 259–287.

(15) Sukpattanacharoen, C.; Kumar, P.; Chi, Y.; Kungwan, N.; Escudero, D. Formation of Excimers in Isoquinolinyl Pyrazolate Pt (II) Complexes: Role of Cooperativity Effects. *Inorg. Chem.* **2020**, *59* (24), 18253-18263.

(16) Bartlett, R. J. How and Why Coupled-Cluster Theory Became the Pre-Eminent Method in an Ab into Quantum Chemistry. In *Theory and Applications of Computational Chemistry*; Elsevier, 2005; pp 1191–1221.

(17) Riplinger, C.; Neese, F. An Efficient and near Linear Scaling Pair Natural Orbital Based Local Coupled Cluster Method. *J. Chem. Phys.* **2013**, *138* (3), 34106.

(18) Riplinger, C.; Sandhoefer, B.; Hansen, A.; Neese, F. Natural Triple Excitations in Local Coupled Cluster Calculations with Pair Natural Orbitals. *J. Chem. Phys.* **2013**, *139* (13), 134101.

(19) Saitow, M.; Becker, U.; Riplinger, C.; Valeev, E. F.; Neese, F. A New Near-Linear Scaling, Efficient and Accurate, Open-Shell Domain-Based Local Pair Natural Orbital Coupled Cluster Singles and Doubles Theory. *J. Chem. Phys.* **2017**, *146* (16), 164105.

(20) Guo, Y.; Riplinger, C.; Becker, U.; Liakos, D. G.; Minenkov, Y.; Cavallo, L.; Neese, F. Communication: An Improved Linear Scaling Perturbative Triples Correction for the Domain Based Local Pair-Natural Orbital Based Singles and Doubles Coupled Cluster Method [DLPNO-CCSD (T)]. *J. Chem. Phys.* **2018**, *148* (1), 11101.

(21) Liakos, D. G.; Guo, Y.; Neese, F. Comprehensive Benchmark Results for the Domain Based Local Pair Natural Orbital Coupled Cluster Method (DLPNO-CCSD (T)) for Closed-and Open-Shell Systems. *J. Phys. Chem. A* **2019**, *124* (1), 90–100.

(22) Chamkin, A. A.; Serkova, E. S. DFT, DLPNO- CCSD (T), and NEVPT2 Benchmark Study of the Reaction between Ferrocenium and Trimethylphosphine. *J. Comput. Chem.* **2020**, *41* (28), 2388–2397.

(23) Shang, Y.; Ning, H.; Shi, J.; Wang, H.; Luo, S.-N. Benchmarking Dual-Level MS-Tor and DLPNO-CCSD (T) Methods for H-Abstraction from Methyl Pentanoate by an OH Radical. *Phys. Chem. Chem. Phys.* **2019**, *21* (37), 20857–20867.

(24) Minenkov, Y.; Chermak, E.; Cavallo, L. Accuracy of DLPNO–CCSD (T) Method for Noncovalent Bond Dissociation Enthalpies from Coinage Metal Cation Complexes. *J. Chem. Theory Comput.* **2015**, *11* (10), 4664–4676.

(25) Paiva, P.; Ramos, M. J.; Fernandes, P. A. Assessing the Validity of DLPNO- CCSD (T) in the Calculation of Activation and Reaction Energies of Ubiquitous Enzymatic Reactions. *J. Comput. Chem.* **2020**, *41* (29), 2459–2468.

(26) Pinter, P.; Strassner, T. Prediction of the Efficiency of Phosphorescent Emitters: A Theoretical Analysis of Triplet States in Platinum Blue Emitters. *Chem. Eur. J.* **2019**, *25* (16), 4202–4205.

(27) Niehaus, T. A.; Hofbeck, T.; Yersin, H. Charge-Transfer Excited States in Phosphorescent Organo-Transition Metal Compounds: A Difficult Case for Time Dependent Density Functional Theory? *RSC Adv.* **2015**, *5* (78), 63318–63329.

(28) Yersin, H.; Rausch, A. F.; Czerwieniec, R.; Hofbeck, T.; Fischer, T. The Triplet State of Organo-Transition Metal Compounds. Triplet Harvesting and Singlet Harvesting for Efficient OLEDs. *Coord. Chem. Rev.* **2011**, *255* (21–22), 2622–2652.

(29) Yersin, H.; Donges, D. Low-Lying Electronic States and Photophysical Properties of Organometallic Pd (II) and Pt (II) Compounds. Modern Research Trends Presented in Detailed Case Studies. *Transit. Met. Rare Earth Compd.* **2001**, 81–186.

(30) Rausch, A. F.; Murphy, L.; Williams, J. A. G.; Yersin, H. Improving the Performance of Pt (II) Complexes for Blue Light Emission by Enhancing the Molecular Rigidity. *Inorg. Chem.* **2012**, *51* (1), 312–319.

(31) Rausch, A. F.; Homeier, H. H. H.; Yersin, H. Organometallic Pt (II) and Ir (III) Triplet Emitters for OLED Applications and the Role of Spin–Orbit Coupling: A Study Based on High-Resolution Optical Spectroscopy. In *Photophysics of Organometallics*; Springer, 2010; pp 193–235.

(32) Gourlaouen, C.; Daniel, C. Spin–Orbit Effects in Square-Planar Pt (II) Complexes with Bidentate and Terdentate Ligands: Theoretical Absorption/Emission Spectroscopy. *Dalt. Trans.* **2014**, *43* (47), 17806–17819.

(33) Zhang, S.; Pattacini, R.; Braunstein, P.; De Cola, L.; Plummer, E.; Mauro, M.; Gourlaouen, C.; Daniel, C. Synthesis, Structure, and Optical Properties of Pt (II) and Pd (II) Complexes with Oxazolyl-and Pyridyl-Functionalized DPPM-Type Ligands: A Combined Experimental and Theoretical Study. *Inorg. Chem.* **2014**, *53* (24), 12739–12756.

(34) Lam, E. S.; Tsang, D. P.; Lam, W. H.; Tam, A. Y.; Chan, M.; Wong, W.; Yam, V. W.

Luminescent Platinum (II) Complexes of 1, 3- Bis (N- alkylbenzimidazol- 2′ - yl) Benzene- Type Ligands with Potential Applications in Efficient Organic Light- Emitting Diodes. *Chem. Eur. J.* **2013**, *19* (20), 6385–6397.

(35) Röhrs, M.; Escudero, D. Multiple Anti-Kasha Emissions in Transition-Metal Complexes. *J. Phys. Chem. Lett.* **2019**, *10* (19), 5798–5804.

(36) Gazzetto, M.; Artizzu, F.; Attar, S. S.; Marchiò, L.; Pilia, L.; Rohwer, E. J.; Feurer, T.; Deplano, P.; Cannizzo, A. Anti-Kasha Conformational Photoisomerization of a Heteroleptic Dithiolene Metal Complex Revealed by Ultrafast Spectroscopy. *J. Phys. Chem. A* **2020**, *124* (51), 10687-10693.

(37) Liu, J.; Yang, C.-J.; Cao, Q.-Y.; Xu, M.; Wang, J.; Peng, H.-N.; Tan, W.-F.; Lü, X.-X.; Gao, X.-C. Synthesis, Crystallography, Phosphorescence of Platinum Complexes Coordinated with 2-Phenylpyridine and a Series of β-Diketones. *Inorganica Chim. Acta* **2009**, *362* (2), 575–579.

(38) Hohenberg, P. P Hys. Rev. 1964, 136, B864–B871; b) w. Kohn, Lj Sham. *Phys. Rev* **1965**, *140*, A1133–A1138.

(39) Parr, R. G. W. Yang Density Functional Theory of Atoms and Molecules. *O xford Univ. Press* **1989**, *1*, 989.

(40) Kohn, W.; Sham, L. J. Self-Consistent Equations Including Exchange and Correlation Effects. *Phys. Rev.* **1965**, *140* (4A), A1133.

(41) Lee, C.; Yang, W.; Parr, R. G. Development of the Colle-Salvetti Correlation-Energy

Formula into a Functional of the Electron Density. *Phys. Rev. B* **1988**, *37* (2), 785.

(42) Becke, A. D. Density- functional Thermochemistry. I. The Effect of the Exchange- only Gradient Correction. *J. Chem. Phys.* **1992**, *96* (3), 2155–2160.

(43) Becke, A. D. Becke's Three Parameter Hybrid Method Using the LYP Correlation Functional. *J. Chem. Phys* **1993**, *98* (492), 5648–5652.

(44) Andrae, D.; Haeussermann, U.; Dolg, M.; Stoll, H.; Preuss, H. Energy-Adjusted Ab Initio Pseudopotentials for the Second and Third Row Transition Elements. *Theor. Chim. Acta* **1990**, *77* (2), 123–141.

(45) Gross, E. K. U.; Dobson, J. F.; Petersilka, M. Density Functional Theory of Time-Dependent Phenomena. *Density Funct. theory II* **1996**, 81–172.

(46) Runge, E.; Gross, E. K. U. Density-Functional Theory for Time-Dependent Systems. *Phys. Rev. Lett.* **1984**, *52* (12), 997.

(47) Casida, M. E. Time-Dependent Density Functional Response Theory for Molecules. In *Recent Advances In Density Functional Methods: (Part I)*; World Scientific, 1995; pp 155–192.

(48) Marques, M. A. L.; Gross, E. K. U. Time-Dependent Density Functional Theory. In *A Primer in Density Functional Theory*; Springer, 2003; pp 144–184.

(49) Frisch, M. J.; Trucks, G. W.; Schlegel, H. B.; Scuseria, G. E.; Robb, M. A.; Cheeseman, J. R.; Scalmani, G.; Barone, V.; Petersson, G. A.; Nakatsuji, H. Gaussian 16, Gaussian. *Inc., Wallingford CT* **2016**, *2016*.

(50) Reiher, M.; Wolf, A. Exact Decoupling of the Dirac Hamiltonian. II. The Generalized Douglas–Kroll–Hess Transformation up to Arbitrary Order. *J. Chem. Phys.* **2004**, *121* (22), 10945–10956.

(51) Lenthe, E. van; Baerends, E.-J.; Snijders, J. G. Relativistic Regular Two- component Hamiltonians. *J. Chem. Phys.* **1993**, *99* (6), 4597–4610.

(52) van Wüllen, C. Molecular Density Functional Calculations in the Regular Relativistic Approximation: Method, Application to Coinage Metal Diatomics, Hydrides, Fluorides and Chlorides, and Comparison with First-Order Relativistic Calculations. *J. Chem. Phys.* **1998**, *109* (2), 392–399.

(53) Neese, F. The ORCA Program System, WIREs Comput. Mol. Sci 2012.

(54) Hirata, S.; Head-Gordon, M. Time-Dependent Density Functional Theory within the Tamm–Dancoff Approximation. *Chem. Phys. Lett.* **1999**, *314* (3–4), 291–299.

(55) Peach, M. J. G.; Warner, N.; Tozer, D. J. On the Triplet Instability in TDDFT. *Mol. Phys.* **2013**, *111* (9–11), 1271–1274.

(56) Peach, M. J. G.; Williamson, M. J.; Tozer, D. J. Influence of Triplet Instabilities in TDDFT. *J. Chem. Theory Comput.* **2011**, *7* (11), 3578–3585.

(57) Wang, Y.; Wu, G. Improving the TDDFT Calculation of Low- lying Excited States for Polycyclic Aromatic Hydrocarbons Using the Tamm–Dancoff Approximation. *Int. J. Quantum Chem.* **2008**, *108* (3), 430–439.

(58) Lee, C.; Yang, W.; Parr, R. G. Density-Functional Exchange-Energy Approximation with

Correct Asymptotic Behaviour. *Phys. Rev. B* **1988**, *37*, 785–789.

(59) Vosko, S. H.; Wilk, L.; Nusair, M. Accurate Spin-Dependent Electron Liquid Correlation Energies for Local Spin Density Calculations: A Critical Analysis. *Can. J. Phys.* **1980**, *58* (8), 1200–1211.

(60) Grimme, S. Semiempirical GGA- type Density Functional Constructed with a Long- range Dispersion Correction. *J. Comput. Chem.* **2006**, *27* (15), 1787–1799.

(61) Yanai, T.; Tew, D. P.; Handy, N. C. A New Hybrid Exchange–Correlation Functional Using the Coulomb-Attenuating Method (CAM-B3LYP). *Chem. Phys. Lett.* **2004**, *393* (1–3), 51–57.

(62) Vydrov, O. A.; Scuseria, G. E.; Perdew, J. P. Tests of Functionals for Systems with Fractional Electron Number. *J. Chem. Phys.* **2007**, *126* (15), 154109.

(63) Perdew, J. P.; Ernzerhof, M.; Burke, K. Rationale for Mixing Exact Exchange with Density Functional Approximations. *J. Chem. Phys.* **1996**, *105* (22), 9982–9985.

(64) Zhao, Y.; Truhlar, D. G. A New Local Density Functional for Main-Group Thermochemistry, Transition Metal Bonding, Thermochemical Kinetics, and Noncovalent Interactions. *J. Chem. Phys.* **2006**, *125* (19), 194101.

(65) Zhao, Y.; Truhlar, D. G. The M06 Suite of Density Functionals for Main Group Thermochemistry, Thermochemical Kinetics, Noncovalent Interactions, Excited States, and Transition Elements: Two New Functionals and Systematic Testing of Four M06-Class Functionals and 12 Other Function. *Theor. Chem. Acc.* **2008**, *120* (1), 215–241.

(66) Zhao, Y.; Truhlar, D. G. Comparative DFT Study of van Der Waals Complexes: Rare-Gas Dimers, Alkaline-Earth Dimers, Zinc Dimer, and Zinc-Rare-Gas Dimers. *J. Phys. Chem. A* **2006**, *110* (15), 5121–5129.

(67) Zhao, Y.; Truhlar, D. G. Density Functional for Spectroscopy: No Long-Range Self-Interaction Error, Good Performance for Rydberg and Charge-Transfer States, and Better Performance on Average than B3LYP for Ground States. *J. Phys. Chem. A* **2006**, *110* (49), 13126–13130.

(68) Haoyu, S. Y.; He, X.; Li, S. L.; Truhlar, D. G. MN15: A Kohn–Sham Global-Hybrid Exchange–Correlation Density Functional with Broad Accuracy for Multi-Reference and Single-Reference Systems and Noncovalent Interactions. *Chem. Sci.* **2016**, *7* (8), 5032–5051.

(69) Biczysko, M.; Panek, P.; Scalmani, G.; Bloino, J.; Barone, V. Harmonic and Anharmonic Vibrational Frequency Calculations with the Double-Hybrid B2PLYP Method: Analytic Second Derivatives and Benchmark Studies. *J. Chem. Theory Comput.* **2010**, *6* (7), 2115–2125.

(70) Zhao, Y.; Truhlar, D. G. Design of Density Functionals That Are Broadly Accurate for Thermochemistry, Thermochemical Kinetics, and Nonbonded Interactions. *J. Phys. Chem. A* **2005**, *109* (25), 5656–5667.

(71) Marenich, A. V; Cramer, C. J.; Truhlar, D. G. Universal Solvation Model Based on Solute Electron Density and on a Continuum Model of the Solvent Defined by the Bulk Dielectric Constant and Atomic Surface Tensions. *J. Phys. Chem. B* **2009**, *113* (18), 6378–6396.

(72) Preston, D. M.; GÜNTNER, W. .; Lechner, A.; Gliemann, G.; Zink, J. I. Unusual Spectroscopic Features in the Emission and Absorption Spectra of Single-Crystal K2 [PtCl4] Caused by Multiple-Mode Excited-State Distortions. *J. Am. Chem. Soc.* **1988**, *110* (17), 5628–5633.

(73) Webb, D. L.; Ancarani Rossiello, L. Luminescence of Platinum (II) Complexes. *Inorg. Chem.* **1971**, *10* (10), 2213–2218.

(74) Donges, D.; Nagle, J. K.; Yersin, H. Characterization of Intraligand Charge Transfer Transitions in Pd (Qol) 2, Pt (Qol) 2 and Pt (Qtl) 2 Investigated by Shpol'skii Spectroscopy. *J. Lumin.* **1997**, *72*, 658–659.

(75) Rausch, A. F.; Monkowius, U. V; Zabel, M.; Yersin, H. Bright Sky-Blue Phosphorescence of [n-Bu4N][Pt (4, 6-DFppy)(CN) 2]: Synthesis, Crystal Structure, and Detailed Photophysical Studies. *Inorg. Chem.* **2010**, *49* (17), 7818–7825.

(76) Yersin, H.; Strasser, J. Triplets in Metal–Organic Compounds. Chemical Tunability of Relaxation Dynamics. *Coord. Chem. Rev.* **2000**, *208* (1), 331–364.

(77) Ma, B.; Djurovich, P. I.; Thompson, M. E. Excimer and Electron Transfer Quenching Studies of a Cyclometalated Platinum Complex. *Coord. Chem. Rev.* **2005**, *249* (13–14), 1501–1510.

(78) Rausch, A. F.; Murphy, L.; Williams, J. A. G.; Yersin, H. Probing the Excited State Properties of the Highly Phosphorescent Pt (Dpyb) Cl Compound by High-Resolution Optical Spectroscopy. *Inorg. Chem.* **2009**, *48* (23), 11407–11414.

(79) Escudero, D.; Thiel, W. Exploring the Triplet Excited State Potential Energy Surfaces of a Cyclometalated Pt (II) Complex: Is There Non-Kasha Emissive Behavior? *Inorg. Chem.* **2014**, *53* (20), 11015–11019.

(80) Chassot, L.; Mueller, E.; Von Zelewsky, A. Cis-Bis (2-Phenylpyridine) Platinum (II)(CBPPP): A Simple Molecular Platinum Compound. *Inorg. Chem.* **1984**, *23* (25), 4249–4253.

(81) Sicilia, V.; Arnal, L.; Escudero, D.; Fuertes, S.; Martin, A. Chameleonic Photo-and Mechanoluminescence in Pyrazolate-Bridged NHC Cyclometalated Platinum Complexes. *Inorg. Chem.* **2021**, *60* (16), 12274-12284.

(82) Mdleleni, M. M.; Bridgewater, J. S.; Watts, R. J.; Ford, P. C. Synthesis, Structure, and Spectroscopic Properties of Ortho-Metalated Platinum (II) Complexes. *Inorg. Chem.* **1995**, *34* (9), 2334–2342.

(83) Fischer, T.; Czerwieniec, R.; Hofbeck, T.; Osminina, M. M.; Yersin, H. Triplet State Properties of a Red Light Emitting [Pt (s-Thpy)(Acac)] Compound. *Chem. Phys. Lett.* **2010**, *486* (1–3), 53–59.

(84) Brooks, J.; Babayan, Y.; Lamansky, S.; Djurovich, P. I.; Tsyba, I.; Bau, R.; Thompson, M. E. Synthesis and Characterization of Phosphorescent Cyclometalated Platinum Complexes. *Inorg. Chem.* **2002**, *41* (12), 3055–3066.

(85) Maestri, M.; Sandrini, D.; Balzani, V.; Chassot, L.; Jolliet, P.; Von Zelewsky, A. Luminescence of Ortho-Metallated Platinum (II) Complexes. *Chem. Phys. Lett.* **1985**, *122* (4), 375–379.

TOC

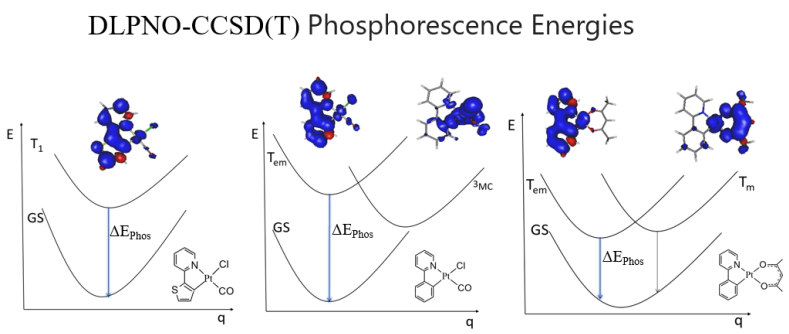
DLPNO-CCSD(T) Phosphorescence Energies
E
T1
GS
ΔEPhos
q
E
Tem
3MC
GS
ΔEPhos
q
E
Tem
Tm
GS
ΔEPhos
q